CT Late Enhancement Segmentation for the Combined Analysis of Coronary Arteries and Myocardial Viability

A.Hennemuth[1] and A. Mahnken[2] and C. Kühnel[1] and S. Oeltze[3] and H.-O. Peitgen[1]

[1]MeVis Research, Bremen, Germany
[2]Radiology Department, University Hospital Aachen, Germany
[3]Department of Simulation and Graphics, University Magdeburg, Germany

Abstract

Non-invasive imaging techniques become more and more important as diagnostic tools for the assessment of coronary heart disease (CHD). While CT is widely applied for the inspection of the coronary arteries, the state of myocardial tissue is normally analyzed with MRI or nuclear imaging methods such as PET or SPECT.

The effect of late enhancement, the accumulation of contrast agent in defective tissue, is used to assess tissue viability with MR imaging. Studies have shown, that this effect can be observed for iodine based contrast agents, which are used for CT coronary artery imaging, as well.

Thus the goal of this work is the development of segmentation and visualization methods, which allow a combined inspection of the coronary arteries and the viability of the corresponding myocardial tissue. We therefore present a new segmentation method for the analysis of CT late enhancement images and the integration with methods for the inspection of the coronary arteries.

In preliminary tests by a radiologist, the methods are applied to 4 datasets to compare the segmentation with the reference method, test the combined inspection for data with a known relation between infarction and supplying artery and test the general applicability to patient data.

The preliminary results are promising, and further studies will focus on the evaluation of the segmentation method as well as on the clinical benefit through the combined analysis.

Categories and Subject Descriptors (according to ACM CCS): I.3.3 [Computer Graphics]: Image processing software

1. Introduction

Coronary heart disease (CHD) is one of the main causes of death in the western world. The disease starts with pathological changes in the vessel walls of the coronary arteries. Different kinds of plaque can cause vessel narrowings or obstructions, which in turn result in a decreased blood supply of the dependent heart muscle, the myocardium. If this hyposupply persists, the myocardial tissue becomes inactive and necrotic, the patient has a myocardial infarction. For diagnosis and therapy planning in CHD, there are two important aspects:

1. The state of the coronary vessel walls
2. The state of the myocardial tissue

An inspection of the coronary arteries provides information about existing plaques, which may cause occlusions and vessel narrowings (stenoses) and thus reduce the blood supply of the dependent tissue. This information is crucial for planning revascularization therapies such as bypass surgery or interventions that aim at reopening the affected vessel like PTCA (percutaneous transluminal coronary angioplasty) and/or stenting (placing a wire mesh tube to prop open the vessel).

The examination of the myocardium allows an assessment of the effect caused by existing or former occlusions or stenoses and thus provides important information for therapy decisions. Only non-necrotic viable myocardium can benefit from revascularization, and interventions are not beneficial, if the tissue, which is supplied by the treated artery, is al-

ready completely infarcted.

While CT becomes more and more established as a means for the non-invasive assessment of the coronary arteries, the viability of myocardial tissue is normally examined with MRI or nuclear imaging technologies such as PET and SPECT.

Studies have shown that the effect of late enhancement, the accumulation of contrast agent in necrotic tissue, can be observed for the iodine based CT contrast agents in the same way as for the gadolinium based contrast agents used for MR viability imaging [GBH*78, MBK*07]. Although the additional amount of radiation applied to the patient is a major drawback, there are certain aspects, which make the late enhancement analysis with CT appealing. To optimally examine the aforementioned interplay between stenoses and ischemia, coronary arteries and myocardium should be examined together. This currently requires the application of different modalities (e.g. CT for the coronaries and PET for the viability analysis), which is not practical for clinical routine. The use of separate scanners is time expensive and the application of hybrid scanners like PET-CT or SPECT-CT is limited by their low availability and their high costs. CT, on the other hand, is widely available and the late enhancement examination does not even require an additional application of contrast agent. Thus, the goal of this work is the development of segmentation methods for the assessment of late enhancement in CT images. To enable a combined inspection of the coronary arteries and the myocardial tissue state, the method is embedded into a prototypical application. Besides the segmentation of the myocardial region that exhibits late enhancement, the prototype allows the segmentation of the coronary arteries. In a third step, we provide visualization and interaction methods for the exploration and assessment of coronary lesions and the viability state of the dependent myocardium.

2. Related Work

This section describes related approaches to the analysis of the late enhancement regions and the combined inspection of coronary arteries and myocardial viability.

2.1. Viability Analysis with Late Enhancement Imaging

Viability assessment with MR imaging is a common method in clinical routine. For the segmentation and quantification of myocardial regions, which show late enhancement, commercially available tools offer basic methods such as thresholding two or three standard deviations above the average intensity value of a healthy myocardial region [KFP*99]. An extension of this method, which applies a combination of both thresholds, is used to further classify infarctions into core and peri-infarct regions [YSB*06].

There exist different approaches to compute a threshold automatically [BPN*03, KCW*05], apply clustering methods [PPG*05], or classify myocardial voxels based on support vector machines [OXSW03].

Due to the so-called *steal phenomenon*, in coronary artery disease infarctions start subendocardially and grow from the inner to the outer part of the myocardium. This fact has been considered in the approach of Hsu et al. [HNK*06], who perform a feature analysis after the initial thresholding. In addition to checking the subendocardial distance, a 3D connectivity analysis is applied to remove false positive segmentations.

For therapy decisions, it is important to know the transmurality, the degree of penetration of myocardium with infarction from endocardium to the outer surface [CKG*01]. For this purpose, many approaches simply determine the portion of segmented voxels per radial segment [NHBR04,PSP*03]. This method does not consider the position of the segmented voxels relative to epi- and endocardium.

The described methods have not been applied to CT images so far, although they might be suitable for this modality as well.

2.2. Combined Inspection of Coronary Arteries and Myocardium

The combined inspection of the coronary arteries and myocardial viability provides important information for therapy planning and assessment. The examination of the coronary arteries and myocardial tissue are normally performed with different modalities. Approaches for the joint assessment of both aspects operate at different levels of abstraction to illustrate correspondences.

Many approaches focus on the multimodal image fusion. Schindler et al. [SMJ*99] propose a method for the fused 3D visualization of results from coronary angiography and myocardial scintigraphy and apply this to pre- and postinterventional image data. A general framework for the fusion of multimodal data is presented by Slomka et al. [Slo04]. The application to the combined visualization of coronary arteries and data from nuclear imaging is shown as an example.

Advanced approaches use image analysis results to provide visualizations, which are specially-tailored to the current problem. Setser et al. [SOS*05] present methods for the fused visualization of MR viability images and coronary arteries from CT images. They show the segmented coronary branches as 3D objects together with the coregistered MR image slices and thus support the assessment of the spatial correspondences.

Approaches that focus on myocardial analysis results fuse information from CT coronary angiography and examinations of the myocardium by superimposing myocardial parameter information with the volume rendering of the CT image data [HMH*06, GSV*07]. Further approaches operate at different levels of abstraction and offer interaction methods for the exploration of image analysis results. Oeltze et al. [OGHP06] apply the standard AHA segmentation [CWD*02] to correlate myocardium related results and coronary artery analysis. Bulls-Eye-Plot segments cor-

responding to regions selected in the coronary artery image are highlighted and contrariwise 3D regions corresponding to the currently selected Bulls-Eye-Plot segments are rotated into focus. Kühnel et al. extend this approach by the possibility to link 3D and 2D image views for the exploration of suspicious image positions [KHO*08]. Termeer et al. [TBB*07] provide a framework for the joint exploration of results from MR whole heart and late enhancement images. Data can be combined and explored at different levels of abstraction like the bulls-eye-plot, surface renderings, overlays and the raw image data.

3. Late Enhancement Segmentation in CT Images

As described by Nieman et al [NSF*08], the intensity difference between hyperenhanced and normal myocardial tissue is significantly lower in CT images than in MR images. Furthermore, CT images tend to be noisy, and the basic application of thresholding methods may result in the segmentation of noisy structures that do not correspond to necrotic tissue. Another important fact to consider for the segmentation of late enhanced myocardium is the subendocardial location. As described by Hsu et al. [HIK*06] this knowledge can be incorporated in the segmentation process.

The proposed method starts with a semi-automatic segmentation of the myocardium with a live wire algorithm [SPP00]. In the next step, the intensity distribution inside the segmented myocardium is analyzed. Two Gaussians, which represent the intensity distribution of healthy(M) and necrotic hyperenhanced(LE) myocardial tissue, are fitted with Expectation Maximization [KP01].

$$h(x) = \underbrace{\alpha_M \frac{1}{\sqrt{2\pi}\sigma_M} e^{-\frac{1}{2}\left(\frac{x-\mu_M}{\sigma_M}\right)^2}}_{\text{Healthy myocardium}} + \underbrace{\alpha_{LE} \frac{1}{\sqrt{2\pi}\sigma_{LE}} e^{-\frac{1}{2}\left(\frac{x-\mu_{LE}}{\sigma_{LE}}\right)^2}}_{\text{Hyperenhanced myocardium}}$$

$$(1)$$

Figure 1 shows an example for the fitting result of a CT dataset of a patient with a known infarction.

From the histogram analysis we derive a partial volume model for the late enhancement quantification. Thereto we assume the following portions $p(x)$ for voxel intensities x:

$$p(x) = \begin{cases} 0 & \text{if } x \leq \mu_M, \\ \frac{x-\mu_M}{\mu_{LE}-\mu_M} & \text{if } \mu_M < x \leq \mu_{LE}, \\ 1 & \text{if } \mu_{LE} < x. \end{cases} \quad (2)$$

To make sure that the segmented regions are connected to the endocardium, the segmentation is initialized with seed voxels v, which fully belong to late enhancement regions according to the partial volume model. Additionally, the seed voxels v have to be located closer to the endocardium (*endo*) than to the epicardium (*epi*):

$$(p(x) = 1) \wedge \left(\frac{d(v, endo)}{d(epi, endo)} \leq 0.5 \right) \quad (3)$$

The segmentation is based on a watershed transform [HP03], because this method separates regions, which are connected
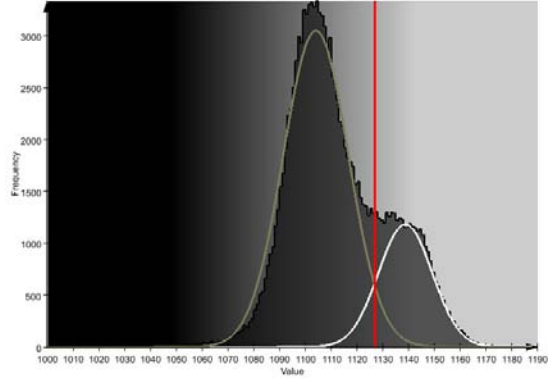
Figure 1: *Analysis of the myocardial intensity distribution in a CT dataset of a patient with an infarction. The histogram is approximated by fitting two Gaussians with Expectation Maximization*

when applying a threshold criterion but have different intensity sinks. This enables a separation of bright regions at the epicardial border which belong to other structures. The seed voxels determined in the previous step are used to define the basins to include into the segmentation. This concept allows an interactive extension by placing additional seedpoints, if the result is not satisfactory.

For the quantification of the late enhanced region the segmentation mask is weighted with the function $p(x)$.

The described methods are integrated into a prototypical application, which is used for the clinical evaluation. The screenshot in Figure 2 shows the user interface for the segmentation. The upper viewers provide possibilities for an interactive manipulation of the segmentation, whereas the lower viewers show different representations of the current segmentation result.

The upper right viewer shows the intensity distribution of the segmented myocardium in yellow. The corresponding color scale is blended in the background. The fitted Gaussians, which represent healthy and necrotic myocardium, are shown in gray and white, whereas the sum of both, which represents the fitting result is blended in dark red. The red bars can be moved by the user to change the segmentation threshold interactively.

The upper left viewer shows the input image. The segmentation overlay can be switched on and off by the user and shows the segmentation result color-coded according to the partial volume model. To extend the segmentation, additional seed voxels can be defined with mouse-clicks. The lower left viewer shows the segmentation result by means of surface rendering. For the generation of the late enhancement surface, we apply the threshold t_s, which corresponds to the intersection of the fitted Gaussians (Fig. 2), if the user does not define another one. The late enhancement surface
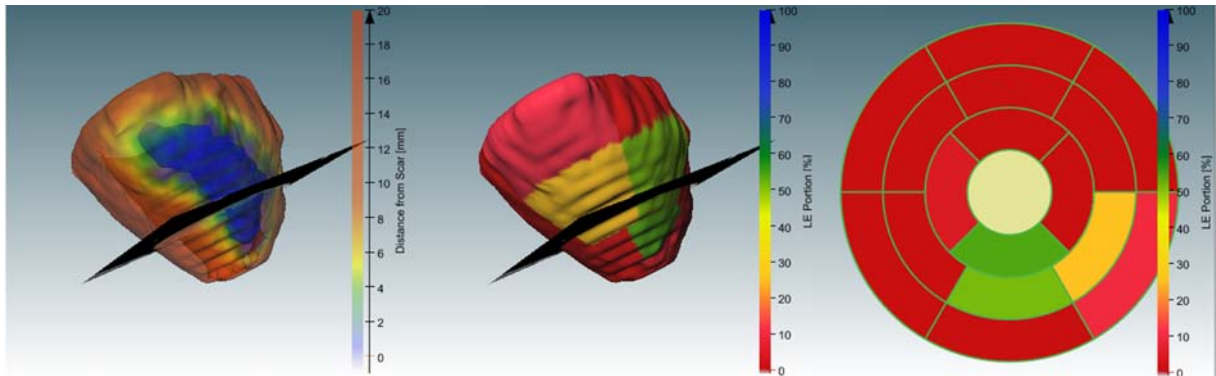
Figure 3: *Correspondence between segmentation result and bulls-eye-plot representation: The leftmost image shows the color-coded surface rendering of the segmentation result. In the middle image the surface is color-coded according to the late enhancement portion per AHA segment. The right image shows the corresponding bulls-eye-plot representation.*
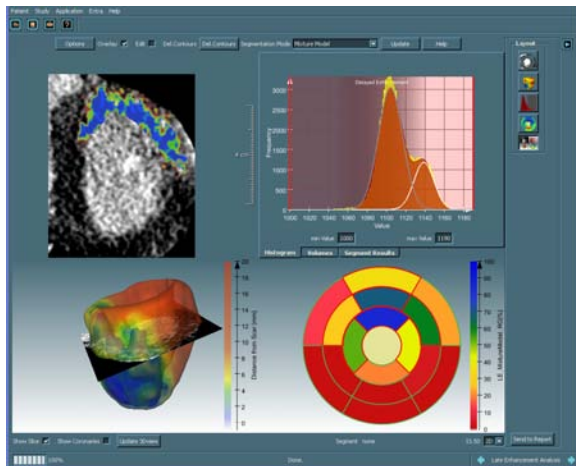
Figure 2: *Software prototype for the late enhancement segmentation: The viewers on the left side show corresponding 2D and 3D visualizations of the segmentation result, whereas the viewers on the left show the underlying intensity distribution as well as the bulls-eye-plot representation of the analysis result.*

is shown in solid dark blue, however the color and opacity of the myocardial surface depends on the distance from the late enhancement region. A red solid color indicates that no late enhanced tissue exists between endocardial and epicardial surface. Transparent blue indicates that the surface is nearly connected to the segmented region. This concept gives an idea of the transmurality of the infarction (see Section 2.1). The lower right viewer shows the segmentation result in the so-called bulls-eye-plot, which is widely used by cardiologists to represent myocardium-related parameters. The portion of late enhancement per AHA-segment is represented in a color scheme, where blue represents 100% whereas red

indicates no late enhancement. The user can switch between the abstract 2D bulls-eye-plot representation and a 3D surface rendering of the segment analysis and thus compare it with the direct 3D surface visualization as shown in Figure 3.

4. Combined Inspection of Coronary Arteries and Myocardial Viability

To enable a combined analysis of late enhancement and coronary arteries, we extend existing concepts for the segmentation and inspection of the coronary arteries. Our prototype performs a semi-automatic coronary tree segmentation [HBB*05].

The next step is dedicated to the interactive inspection of the segmented coronaries and the late enhancement as shown in Figure 4.

The viewers are organized in three groups according to
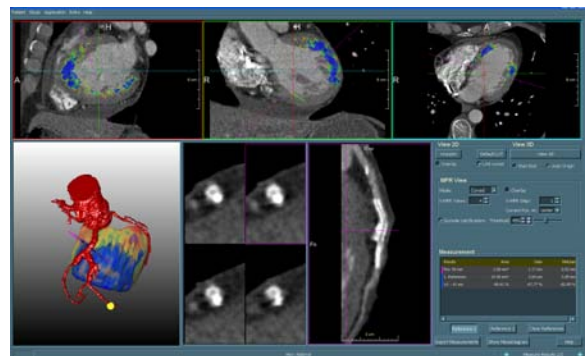
Figure 4: *Prototypical application for the combined inspection of coronary arteries and late enhancement segmentation. The yellow 3D marker in the 3D viewer indicates the selected coronary branch, which is shown in the reformatted views on the right.*

Pat.	Scanner	Scan	Peak voltage [kV]	Tube current [mA]	Exposure time [s]	Exposure [mAs]	Recon. kernel
1	Sensation 16	LE	120	371	303	400	B30f
Pig	Definition	CA	120	1212	330	400	B26f
		LE	120	1212	330	400	B20f
2	Sensation 16	CA	120	371	303	550	B30f
		LE	80	371	303	550	B20f
3	Definition	CA	140	502	330	164	B26f
		LE	120	819	330	269	B30f

Table 1: *Scan parameters of the examined CT coronary angiograms (CA) and late enhancement images (LE). The number in the definition of the reconstruction kernel indicates the degree of smoothing. The lower this value is, the smoother is the reconstructed image.*

different exploration concepts. The upper row shows three orthogonal views of the image volume (sagittal, coronal, axial) for the coronary artery segmentation. The segmentation result of the late enhancement analysis can be shown as an overlay, which is colored according to the partial volume model described in Section 3.

The lower left viewer shows a 3D representation of the segmentation results. The coronary tree is shown by means of volume rendering, whereas the myocardium and late enhancement are visualized as described in Section 3. This view does not only provide an overview of the spatial relations in 3D, but also allows for an interactive definition of the curved MPR on the right. Thereto the user has to select a coronary branch by either placing a 3D marker at the distal end the vessel or by defining start and endpoint of the interesting coronary segment. The corresponding curved MPR is then shown on the right. In this view, the user can place cross MPRs for the analysis of the vessel diameter and profile. The inspected position is shown in the orthogonal views and the 3D view as well and thus it is possible to visually correlate the stenosis and the dependent myocardium.

5. Preliminary Results

In an ongoing study a radiologist applied the methods to three patient datasets acquired with a 16-slice scanner (Siemens Sensation 16) and a 64-slice scanner (Siemens Definition) and one animal dataset acquired with a 64-slice scanner (Siemens Definition). The scan parameters of the datasets are shown in Table 1. The images are used to assess the developed late enhancement segmentation method, the combined inspection and the applicability to patient data.

5.1. Late Enhancement Segmentation

For one patient late enhancement images from CT and MRI are available, so the results of the described segmentation

method can be compared with the reference method. The MR image was acquired with a 1.5T scanner (Philips Intera Achieva) with an in-plane resolution of 1.48×1.48 mm^2 a slice thickness of 8 mm and a gap of 2 mm. CT image data was reconstructed in short-axis orientation, an in-plane resolution of 0.35×0.35 mm^2 and a slice thickness of 8 mm. The CT images are segmented with the new method whereas MR images were segmented manually. For both segmentations the late enhancement volume portions are calculated per AHA-segment. Figure 5 shows the images and segmentation results, which correspond well for CT and MR image analysis

5.2. Combined Inspection or Coronary Arteries and Myocardial Viability

The pig examined with the 64-slice scanner has an inflicted infarction, so the inducing artery as well as the location of the infarction are known. The image data consist of an angiogram that is reconstructed with a resolution of $0.39 \times 0.39 \times 1$ mm^3 and the late enhancement image, which is reconstructed with a resolution of $0.35 \times 0.35 \times 8$ mm^3. Figure 6 shows the combined visualization of the coronaries and the late enhancement segmentation result. The vessel that was occluded to generate the infarction is selected in the 3D view and the cross MPR is defined near the infarction. With the segmentation overlay from the late enhancement analysis the correspondence between the occluded artery and the region that exhibits late enhancement is clearly visible in all provided views.

5.3. Application to Patient Data

Two patient datasets that were acquired with a 16-slice scanner (Siemens Sensation 16) are examined with the methods described in Section 3 and Section 4 (see table 2).
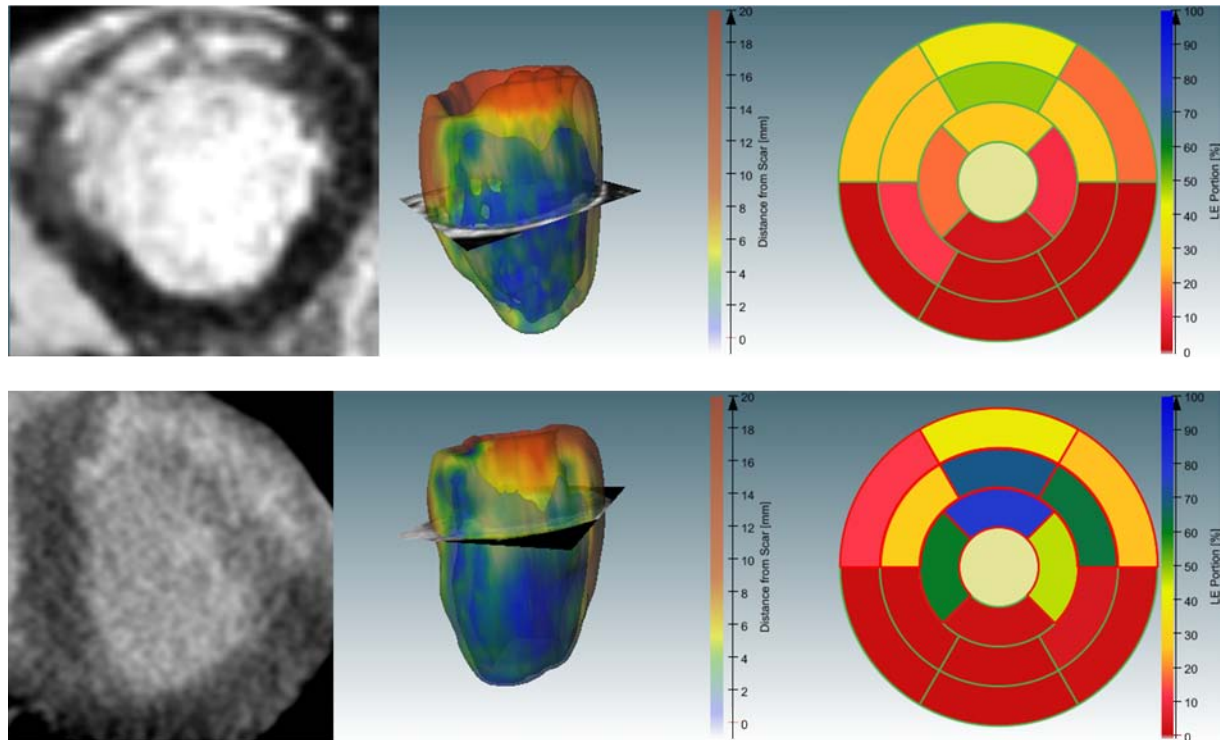
Figure 5: *Late enhancement segmentation results from MRI (upper row) and CT (lower row) for patient 1*

In both datasets, late enhancement regions are detected by

Table 2: *Patient datasets for the combined inspection of the coronary arteries and the viability of the dependent tissue. The angiograms are reconstructed in axial orientation whereas the late enhancement images have short-axis orientation.*

Pat.	Coronary Angiogram Res. (mm,mm,mm)	Late Enhancement Image Res. (mm,mm,mm)
2	(0.43,0.43,0.50)	(0.43,0.43,4.00)
3	(0.35,0.35,0.60)	(0.35,0.35,8.00)

the automatic segmentation. The segmentation of the main coronary branches is possible with additional user interaction. The exploration of the segmentation results is performed by a subsequent selection of the main coronary branches. After the selection in the 3D view, suspicious regions are marked in the curved MPR view and the vessel cross section as well as the adjoining myocardium are examined in the reformatted views. Figure 7 shows screenshots of this inspection. For patient 2 the portion of late enhanced myocardium is relatively small. This region is located adjoining the left anterior descending artery (LAD), which exhibits a fairly large quantity of plaque. Due to its size the

late enhancement region of patient 3 can not clearly be related to one coronary branch. The LAD, which contains a stent is certainly responsible for the supply of a part of the late enhanced region. Whether branches of the left circumflex artery (LCX) have also caused an undersupply can not be decided reliably based on the given visualization.

6. Discussion and Conclusions

In the previous sections we have described a new method for the segmentation of late enhancement regions in CT images to allow a combination of coronary artery inspection with a viability analysis of the dependent myocardial tissue. Thereto we extend visualization and interaction concepts for the exploration of results from coronary artery and late enhancement segmentation results. Starting from a 3D representation the user can select coronary segments that are visualized in different linked MPR views, where the overlay of the late enhancement segmentation provides information about the state of myocardial tissue next to an eventually detected lesion.

The preliminary tests performed by a radiologist show promising results for the examined datasets. The expert appreciated the presented software prototypes as helpful innovative tools, but the limited amount of inspected datasets
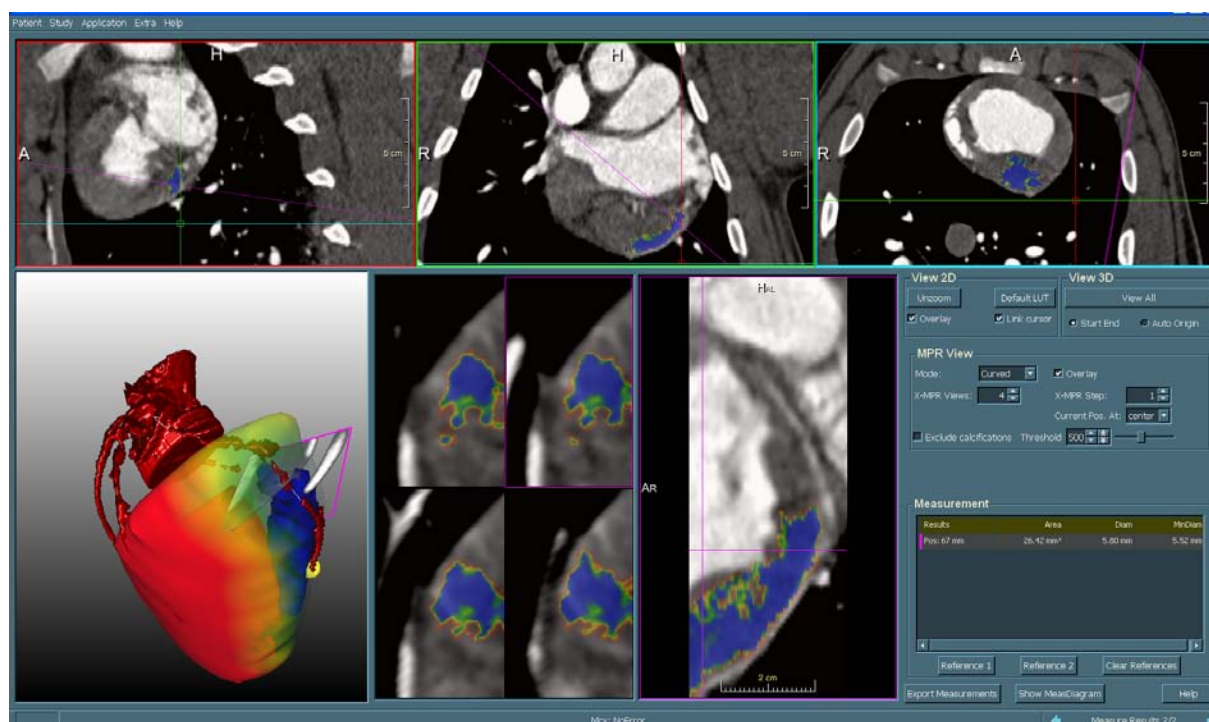
Figure 6: *Combined visualization for the animal dataset: In the application screenshot the correspondence between the segmented late enhancement region and the selected temporarily occluded artery is clearly visible.*

does not allow a definite conclusion about the clinical applicability yet.

The examined late enhancement scans, which were acquired with the Siemens Definition scanner applied a radiation dose of ca. 5.5 mSV. In a clinical setting this could be reduced to 2mSV by means of prospective gating. Further studies will have to test the segmentation methods for different scan protocols. Furthermore, it is likely, that a registration of the angiogram and the late enhancement image will be necessary in other datasets, because there is an interval of at least ten minutes between the scans and the patient may move or hold the breath in another inspiration phase in the second scan.

The described methods are integrated in prototypical software applications in order to enable clinical studies of the benefit through the proposed combined inspection.

References

[BPN*03] BREEUWER M., PAETSCH I., NAGEL E., MUTHUPILLAI R., FLAMM S., PLEIN S.: The detection of normal, ischemic and infarcted myocardial tissue using MRI. In *Proceedings of the 17th International Congress and Exhibition on Computer Assisted Radiology and Surgery (CARS'03)* (2003).

[CKG*01] CHOI K., KIM R., GUBERNIKOFF G., VARGAS J., PARKER M., JUDD R.: Transmural extent of acute myocardial infarction predicts long-term improvement in contractile function. *Circulation 104*, 10 (2001), 1101–1107.

[CWD*02] CERQUEIRA M., WEISSMAN N., DILSIZIAN V., JACOBS A., KAUL S., LASKEY W., PENNELL D., RUMBERGER J., RYAN T., VERANI M.: Standardized myocardial segmentation and nomenclature for tomographic imaging of the heart: a statement for healthcare professionals from the cardiac imaging committee of the council on clinical cardiology of the american heart association. *Circulation 105*, 4 (2002), 539–542.

[GBH*78] GRAY W. R., BUJA L. M., HAGLER H. K., PARKEY R. W., WILLERSON J. T.: Computed tomography for localization and sizing of experimental acute myocardial infarcts. *Circulation 58*, 3 Pt 1 (Sep 1978), 497–504.

[GSV*07] GAEMPERLI O., SCHEPIS T., VALENTA I., HUSMANN L., SCHEFFEL H., DUERST V., EBERLI F. R., LUSCHER T. F., ALKADHI H., KAUFMANN P. A.: Cardiac image fusion from stand-alone SPECT and CT: clinical experience. *J Nucl Med 48*, 5 (2007), 696–703.

[HBB*05] HENNEMUTH A., BOCK S., BOSKAMP T., FRITZ D., KUEHNEL C., RINCK D., SCHEUERING

<div align="center">Patient 2   Patient 3</div>

RCA

LAD

LCX
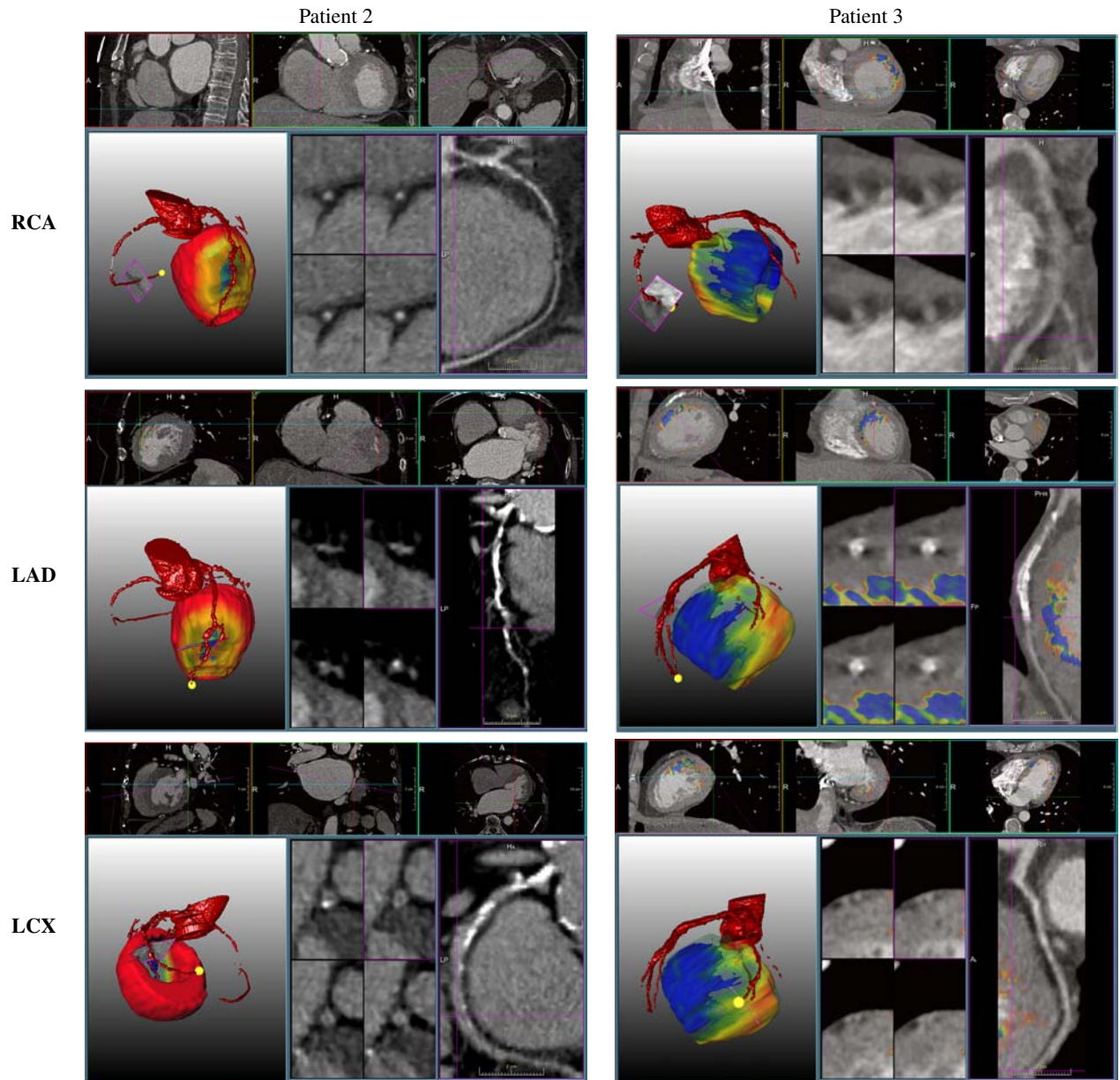
Figure 7: *Combined inspection of the segmentation results for patient 2 and patient 3: The main coronary branches right coronary artery (RCA), left anterior descending (LAD) and left circumflex artery (LCX) are selected in the 3D view (yellow marker) and further explored in the reformatted image views. The late enhancement segmentation result is reformatted and shown as an overlay in all 2D views.*

M.: One-click coronary tree segmentation in CT angiographic images. In *Proceedings of the 19th International Congress and Exhibition on Computer Assisted Radiology and Surgery (CARS'05)* (2005), pp. 317–321.

[HIK*06] HSU L., INGKANISORN W., KELLMAN P., ALETRAS A., ARAI A.: Quantitative myocardial in-farction on delayed enhancement MRI. part II: Clinical application of an automated feature analysis and combined thresholding infarct sizing algorithm. *J Magn Reson Imaging 23* (2006), 309–314.

[HMH*06] HIGASHINO H., MOCHIZUKI T., HARAIKAWA T., KURATA A., KIDO T., NAKATA

S., SUGAWARA Y., MIYAGAWA M., MIKI H., KOYAMA Y., OKAYAMA H., HIGAKI J.: Image fusion of coronary tree and regional cardiac function image using multislice computed tomography. *Circ J 70*, 1 (Jan 2006), 105–109.

[HNK*06] HSU L., NATANZON A., KELLMAN P., HIRSCH G., ALETRAS A., ARAI A.: Quantitative myocardial infarction on delayed enhancement MRI, part I: animal validation of an automated feature analysis and combined thresholding infarct sizing algorithm. *J Magn Reson Imaging 23* (2006), 298–308.

[HP03] HAHN H., PEITGEN H.: Iwt – interactive watershed transform: A hierarchical method for efficient interactive and automated segmentation of multidimensional grayscale images. In *SPIE Medical Imaging 2003* (2003), vol. 5032, SPIE Press, pp. 643–653.

[KCW*05] KOLIPAKA A., CHATZIMAVROUDIS G., WHITE R., O'DONNELL T., SETSER R.: Segmentation of non-viable myocardium in delayed enhancement magnetic resonance images. *Int J Cardiovasc Imaging 21*, 2–3 (2005), 303–311.

[KFP*99] KIM R., FIENO D., PARRISH T., HARRIS K., CHEN E. L., SIMONETTI O., BUNDY J., FINN J., KLOCKE F., JUDD R.: Relationship of MRI delayed contrast enhancement to irreversible injury, infarct age, and contractile function. *Circulation 100*, 19 (1999), 1992–2002.

[KHO*08] KÜHNEL C., HENNEMUTH A., OELTZE S., BOSKAMP T., PEITGEN H.-O.: Enhanced cardio vascular image analysis by combined representation of results from dynamic mri and anatomic cta. In *SPIE Conference on Medical Image Computing 2008* (2008).

[KP01] KIM D., PARK D.: Fast iterative computation of Gaussian mixture parameters and optimal image segmentation. *International Journal of Systems Science 32*, 8 (2001), 1075–1087.

[MBK*07] MAHNKEN A. H., BRUNERS P., KINZEL S., KATOH M., MÜHLENBRUCH G., GÜNTHER R. W., WILDBERGER J. E.: Late-phase msct in the different stages of myocardial infarction: animal experiments. *Eur Radiol 17*, 9 (Sep 2007), 2310–2317.

[NHBR04] NOBLE N., HILL D., BREEUWER M., RAZAVI R.: The automatic identification of hibernating myocardium. In *Proceedings of the 7th International Conference on Medical Image Computing and Computer-Assisted Intervention (MICCAI'04)* (2004), pp. 890–898.

[NSF*08] NIEMAN K., SHAPIRO M. D., FERENCIK M., NOMURA C. H., ABBARA S., HOFFMANN U., GOLD H. K., JANG I.-K., BRADY T. J., CURY R. C.: Reperfused myocardial infarction: contrast-enhanced 64-section ct in comparison to mr imaging. *Radiology 247*, 1 (Apr 2008), 49–56.

[OGHP06] OELTZE S., GROTHUES F., HENNEMUTH A.,

PREIM B.: Integrated visualization of morphologic and perfusion data for the analysis of coronary artery disease. In *Eurographics / IEEE VGTC Symposium on Visualization* (2006), vol.

[OXSW03] O'DONNELL T., XU N., SETSER R., WHITE R.: Semi-automatic segmentation of nonviable cardiac tissue using cine and delayed enhancement magnetic resonance images. *Proceedings of SPIE 5031* (2003), 242.

[PPG*05] POSITANO V., PINGITORE A., GIORGETTI A., FAVILLI B., SANTARELLI M., LANDINI L., MARZULLO P., LOMBARDI M.: A fast and effective method to assess myocardial necrosis by means of contrast magnetic resonance imaging. *Journal of Cardiovascular Magnetic Resonance 7*, 2 (2005), 487–494.

[PSP*03] POSITANO V., SANTARELLI M., PINGITORE A., LOMBARDI M., LANDINI L., BENASSI A.: Quantitative 3D assessment of myocardial viability with MRI delayed contrast enhancement. In *Proceedings of the 30th Annual Conference on Computers in Cardiology (CARS'03)* (2003), pp. 629–632.

[Slo04] SLOMKA P.: Software approach to merging molecular with anatomic information. *J Nucl Med 45*, suppl 1 (2004), 36S–45S.

[SMJ*99] SCHINDLER T., MAGOSAKI N., JESERICH M., OSER U., KRAUSE T., FISCHER R., MOSER E., NITZSCHE E., ZEHENDER M., JUST H.: Fusion imaging: combined visualization of 3d reconstructed coronary artery tree and 3d myocardial scintigraphic image in coronary artery disease. *Int J Card Imaging 15*, 5 (1999), 357–368.

[SOS*05] SETSER R., O'DONNELL T., SMEDIRA N., SABIK J., HALLIBURTON S., STILLMAN A., WHITE R.: Coregistered MR imaging myocardial viability maps and multi-detector row CT coronary angiography displays for surgical revascularization planning: initial experience. *Radiology 237*, 2 (2005), 465–473.

[SPP00] SCHENK A., PRAUSE G., PEITGEN H.-O.: Efficient semiautomatic segmentation of 3D objects in medical images. In *Proceedings of the 3rd International Conference on Medical Image Computing and Computer-Assisted Intervention (MICCAI'00)* (2000), pp. 186–195.

[TBB*07] TERMEER M., BESCÃŞS J. O., BREEUWER M., VILANOVA A., GERRITSEN F., GRÃŬLLER E.: Covicad: comprehensive visualization of coronary artery disease. *IEEE Trans Vis Comput Graph 13*, 6 (2007), 1632–1639.

[YSB*06] YAN A., SHAYNE A., BROWN K., GUPTA S. N., CHAN C., LUU T., CARLI M., REYNOLDS H., STEVENSON W., KWONG R.: Characterization of the peri-infarct zone by contrast-enhanced cardiac magnetic resonance imaging is a powerful predictor of post-myocardial infarction mortality. *Circulation 114*, 1 (2006), 32–39.